Modified PUMA/EPUMA based on Forward and Backward Linear Prediction for DOA Estimation

Biyun Ma, Fu Zhu, Yide Wang, Qingqing Zhu, Jiaojiao Liu

Modified PUMA/EPUMA based on Forward and Backward Linear Prediction for DOA Estimation

Biyun Ma, Fu Zhu, Yide Wang, *Senior Member, IEEE*, Qingqing Zhu, Jiaojiao Liu

***Abstract*—The principal-singular-vector utilization for modal analysis (PUMA) and its modification (Mod-PUMA), which utilize forward linear prediction (FLP) to process the signal subspace, experience significant performance degradation if there are multiple coherent sources and such a performance degradation will be further aggravated in low SNR regions, which is primarily attributed to the outliers arising from inaccurate estimations of the signal subspace. To address these issues, we propose an extension version of PUMA-related algorithms, called FBLP-Mod-PUMA/EPUMA. The proposed algorithms improve the threshold performance by refining the signal subspace through forward and backward linear prediction (FBLP), effectively mitigating subspace leakage when dealing with coherent sources. The number of resolvable coherent sources has been theoretically derived and simulation results are provided to show the performance of the proposed algorithms.**

***Index Terms*—PUMA/EPUMA, DOA estimation, forward and backward linear prediction, coherent sources.**

I. Introduction

THE subspace-based direction-of-arrival (DOA) finding methods, such as MUSIC [1], ESPRIT [2] and their variants, offer significant advantages in terms of computational complexity and resolution capability compared to the maximum likelihood (ML) method and beamforming-based methods, respectively. However, when dealing with coherent sources, these algorithms require decorrelation techniques for preprocessing, such as spatial smoothing (SS) and modified spatial smoothing preprocessing (MSSP) [3], which substantially reduces the effective aperture of the sensor array. To address this, alternative approaches like the method of direction estimation (MODE) [4] and its extension, MODE with extra-roots (MODEX) [5], have been proposed. The MODEX algorithm applies the MODE method twice, once assuming the number of incoming signals is K (the true number of sources) and once assuming it is P ($P > K$), then selects K DOAs from the combined $P+K$ candidate DOAs using a ML based cost function [6]. These methods can handle coherent sources with additional symmetry constraints on the root polynomial coefficients.

Thanks to the National Key Research and Development Program of China under Grant No.2024YFE0105400, the Natural Science Foundation of Guangdong Province of China under Grant No.2023A1515011420, and the National Natural Science Foundation of China under Grant No. 62192711. Biyun Ma, Fu Zhu, Qingqing Zhu, and Jiaojiao Liu are with the School of Electronics and Information Engineering, South China University of Technology, 510640 Guangzhou, China, and Key Laboratory of Marine Environmental Survey Technology and Application, Ministry of Natural Resources, Guangzhou, 510300. (e-mail: eebyma@scut.edu.cn; 202320111612@mail.scut.edu.cn; eeqqzhu@mail.scut.edu.cn; jjliu@scut.edu.cn) Yide Wang is with the Institut d'Electronique et des Technologies du NumeRique (IETR), CNRS UMR6164, Nantes University, 44306 Nantes, France. (e-mail: yide.wang@univ-nantes.fr) Corresponding author: Jiaojiao Liu (e-mail: jjliu@scut.edu.cn).

The principal-singular-vector utilization for modal analysis (PUMA) [7] and enhanced-PUMA (EPUMA) [8] algorithms are improved implementations of MODE and MODEX, respectively, with no additional assumptions or constraints on polynomial coefficients. Furthermore, it has been shown [9] that MODEX and EPUMA share an equivalent cost function. PUMA has a wide range of applications in ocean and water remote sensing environments, which are characterized by challenges, such as signal coherence, time delay, Doppler effects, multipath propagation, and low SNR [10]. However, PUMA and EPUMA are based on the assumption of a full-rank source covariance matrix, which reconstructs the signal subspace using the eigenvectors corresponding to the K (number of sources) largest eigenvalues. This assumption, however, becomes invalid when dealing with coherent sources. To address this limitation, a modified version of PUMA/EPUMA, referred to as Mod-PUMA/EPUMA, was proposed in [11] [12]. Mod-PUMA reconstructs the signal subspace using the eigenvectors corresponding to the N_r largest eigenvalues, where N_r is the actual rank of the source covariance matrix. Moreover, Mod-EPUMA employs a two-step selection strategy based on the stochastic maximum likelihood (Sto-ML) criterion, further enhancing its performance. Moreover, when dealing with multiple coherent sources, where $N_r < K$, the computational complexity of Mod-PUMA/EPUMA is reduced compared to PUMA/EPUMA, attributable to the utilization of a reduced set of signal eigenvectors.

Furthermore, with forward-backward spatial smoothing (FBSS), PUMA/EPUMA and Mod-PUMA/EPUMA achieve a 3 dB improvement in threshold performance. However, the MODE/MODEX with FBSS is asymptotically statistically less efficient than the MODE/MODEX without FBSS [13], especially when the signal covariance matrix is non-diagonal (i.e., the signals are correlated), highlighting that PUMA and Mod-PUMA experience performance degradation in scenarios involving multiple coherent sources. To address the limitations of PUMA/EPUMA, an extension of Mod-PUMA/EPUMA based on forward and backward linear prediction (FBLP), called FBLP-Mod-PUMA/EPUMA, was developed in this paper. The FBLP is applied to overcome the challenges associated with coherent signal processing without additional preprocessing steps that potentially diminish the effective aperture of the sensor array and result in asymptotically statistically less efficient estimation of the signal subspace. As a result, the proposed algorithms achieve superior performance in resolving coherent signals, particularly in low SNR regions. The simulation results are provided to show the effectiveness of the proposed algorithms.

II. System Model

Suppose there are K narrowband sources incident on a uniform linear array (ULA) with N ($K < N$) sensors from K different directions $(\theta_1, \theta_2, \ldots, \theta_K)$, where K is known. So,

$$\mathbf{y}(t) = \mathbf{A}\mathbf{s}(t) + \mathbf{n}(t), \quad 1 \le t \le M \tag{1}$$

where $\mathbf{y}(t) = [y_1(t), y_2(t), \ldots, y_N(t)]^T \in \mathbb{C}^{N\times 1}$ represents the received signal vector, $\mathbf{s}(t) = [s_1(t), s_2(t), \ldots, s_K(t)]^T \in \mathbb{C}^{K\times 1}$ denotes the source signal vector, $\mathbf{n}(t) = [n_1(t), n_2(t), \ldots, n_N(t)]^T \in \mathbb{C}^{N\times 1}$ is the noise vector with zero mean and covariance matrix $\sigma^2\mathbf{I}_N$, where σ^2 is the noise power and $\mathbf{I}_N \in \mathbb{C}^{N\times N}$ is the identity matrix. The noise is assumed to be uncorrelated with $\mathbf{s}(t)$. $\mathbf{A} = [\mathbf{a}(\theta_1), \mathbf{a}(\theta_2), \ldots, \mathbf{a}(\theta_K)] \in \mathbb{C}^{N\times K}$ is the steering matrix, where $\mathbf{a}(\theta) = \left[1, e^{j\pi\sin(\theta)}, \ldots, e^{j\pi(N-1)\sin(\theta)}\right]^T \in \mathbb{C}^{N\times 1}$ denotes the steering vector. M represents the number of snapshots. The covariance matrix of $\mathbf{y}(t)$ is

$$\mathbf{\Gamma} = E[\mathbf{y}(t)\mathbf{y}^H(t)] = \mathbf{A}\mathbf{\Gamma}_s\mathbf{A}^H + \sigma^2\mathbf{I}_N \tag{2}$$

where $\mathbf{\Gamma}_s = E\left[\mathbf{s}\mathbf{s}^H\right] \in \mathbb{C}^{K\times K}$ denotes the source covariance matrix and $1 \le rank(\mathbf{\Gamma}_s)$=$N_r \le K$.

III. Forward and Backward Linear Prediction Modified PUMA/EPUMA

A. Modified PUMA/EPUMA Model

The eigenvalue decomposition of $\mathbf{\Gamma}$ in (2) can be written as,

$$\begin{aligned}\mathbf{\Gamma} &= \mathbf{A}\mathbf{\Gamma}_s\mathbf{A}^H + \sigma^2\mathbf{I}_N = \sum_{i=1}^{N}\eta_i\mathbf{u}_i\mathbf{u}_i^H \\ &= \mathbf{E}_s\mathbf{\Lambda}_s\mathbf{E}_s^H + \sigma^2\mathbf{I}_N = \mathbf{E}_s\mathbf{D}_s\mathbf{E}_s^H + \mathbf{E}_n\mathbf{D}_n\mathbf{E}_n^H\end{aligned} \tag{3}$$

where η_i is the i^{th} largest eigenvalue in $\mathbf{\Gamma}$, where $\eta_i = \lambda_i + \sigma^2, 1 \le i \le N_r$, $\eta_i = \sigma^2, N_r + 1 \le i \le N$. The columns of $\mathbf{E}_s = [\mathbf{u}_1, \ldots, \mathbf{u}_{N_r}]$ are the eigenvectors associated with the N_r largest eigenvalues in $\mathbf{D}_s = diag\left(\lambda_1+\sigma^2, \ldots, \lambda_{N_r}+\sigma^2\right) \in \mathbb{R}^{N_r\times N_r}$, they span the signal subspace. The columns of $\mathbf{E}_n = [\mathbf{u}_{N_r+1}, \ldots, \mathbf{u}_N]$ are the eigenvectors associated with the N-N_r smallest eigenvalues in $\mathbf{D}_n = diag(\sigma^2, \ldots, \sigma^2) \in \mathbb{R}^{(N\text{-}N_r)\times(N\text{-}N_r)}$, they span the noise subspace.

By (3), the following equation could be obtained,

$$\mathbf{A}\mathbf{\Gamma}_s\mathbf{A}^H = \mathbf{E}_s\mathbf{\Lambda}_s\mathbf{E}_s^H \tag{4}$$

$$\mathbf{A}\mathbf{T}\mathbf{T}^H\mathbf{A}^H = \mathbf{E}_s\mathbf{\Lambda}_s^{1/2}\mathbf{\Lambda}_s^{H/2}\mathbf{E}_s^H \tag{5}$$

where $\mathbf{A}$ is a Vandermonde matrix, so

$$\mathbf{B}\mathbf{A} = \mathbf{0}_{(N\text{-}K,K)} \tag{6}$$

$$\mathbf{B} = \begin{bmatrix} c_K & c_{K\text{-}1} & \ldots & c_0 & 0 & 0 & \ldots & 0 \\ 0 & c_K & \ldots & \ldots & c_0 & \ldots & \ldots & \vdots \\ \vdots & \vdots & \ddots & \ddots & \ddots & \ddots & \ddots & \vdots \\ 0 & 0 & \ldots & 0 & c_K & c_{K\text{-}1} & \ldots & c_0 \end{bmatrix}_{(N\text{-}K,N)} \tag{7}$$

where c_0=1. (6) means that the l^{th} element ($l \ge K$+1) of each column of $\mathbf{A}$ is a linear combination of the K previous elements of the same column, which can be expressed as

$$z_k^l + \sum_{i=1}^{K} c_i z_k^{l\text{-}i} = 0, \quad 1 \le k \le K, K\text{+}1 \le l \le N \tag{8}$$

where $z_k = e^{j\pi\sin\theta_k}$. From (5) and (6), $\mathbf{B}\mathbf{A}\mathbf{T}_1 = \mathbf{B}\mathbf{E}_s = \mathbf{B}[\mathbf{u}_1, \mathbf{u}_2, \ldots, \mathbf{u}_{N_r}] = \mathbf{0}_{(N\text{-}K,N_r)}$, thus, the k^{th} column of $\mathbf{E}_s$ has the following forward linear prediction (FLP) property,

$$[\mathbf{u}_k]_l + \sum_{i=1}^{K} c_i[\mathbf{u}_k]_{l\text{-}i} = 0, \quad 1 \le k \le N_r, K\text{+}1 \le l \le N \tag{9}$$

which can be rewritten as

$$\mathbf{F}_{f_k}\mathbf{c} - \mathbf{g}_{f_k} = \mathbf{0}_{(N\text{-}K,1)}, \quad 1 \le k \le N_r \tag{10}$$

where

$$\begin{aligned}\mathbf{F}_{f_k} &= \begin{bmatrix} [\mathbf{u}_k]_K & [\mathbf{u}_k]_{K\text{-}1} & \ldots & [\mathbf{u}_k]_1 \\ [\mathbf{u}_k]_{K+1} & \ldots & \ldots & [\mathbf{u}_k]_2 \\ \vdots & \ddots & \ddots & \vdots \\ [\mathbf{u}_k]_{N\text{-}1} & \ldots & \ldots & [\mathbf{u}_k]_{N\text{-}K} \end{bmatrix}_{(N\text{-}K,K)} \\ \mathbf{g}_{f_k} &= -\begin{bmatrix} [\mathbf{u}_k]_{K+1} & \ldots & [\mathbf{u}_k]_N \end{bmatrix}^T_{(N\text{-}K,1)}\end{aligned} \tag{11}$$

so,

$$\mathrm{vec}(\mathbf{B}\mathbf{E}_s) = \mathbf{F}_F\mathbf{c} - \mathbf{g}_F = \mathbf{0}_{(N_r(N\text{-}K),1)} \tag{12}$$

where $\mathrm{vec}(\cdot)$ is the vectorization operator, and

$$\begin{aligned}\mathbf{F}_F &= \begin{bmatrix} \mathbf{F}_{f_1}^T & \cdots & \mathbf{F}_{f_{N_r}}^T \end{bmatrix}^T_{(N_r(N\text{-}K),K)} \\ \mathbf{g}_F &= \begin{bmatrix} \mathbf{g}_{f_1}^T & \cdots & \mathbf{g}_{f_{N_r}}^T \end{bmatrix}^T_{(N_r(N\text{-}K),1)}\end{aligned} \tag{13}$$

B. FBLP-Mod-PUMA/EPUMA

Mod-PUMA/EPUMA are based on FLP. To further improve the threshold performance in case of coherent sources, an extension of Mod-PUMA/EPUMA based on FBLP is proposed. Similar to (8), by the backward linear prediction (BLP), the l^{th} element ($l \le N$-K) of each column of $\mathbf{A}$ is a linear combination of the K following elements of the same column,

$$(z_k^*)^l + \sum_{i=1}^{K} c_i(z_k^*)^{l+i} = 0, \quad 1 \le k \le K, 1 \le l \le N\text{-}K, \tag{14}$$

So the k^{th} column of $\mathbf{E}_s^*$ is as follows,

$$[\mathbf{u}_k^*]_l + \sum_{i=1}^{K} c_i[\mathbf{u}_k^*]_{l+i} = 0, \quad 1 \le k \le N_r, 1 \le l \le N\text{-}K \tag{15}$$

where $(\cdot)^*$ is the complex conjugate, so (15) can be rewritten,

$$\mathbf{F}_{b_k}\mathbf{c} - \mathbf{g}_{b_k} = \mathbf{0}_{((N\text{-}K),1)}, \quad 1 \le k \le N_r \tag{16}$$

where

$$\begin{aligned}\mathbf{F}_{b_k} &= \begin{bmatrix} [\mathbf{u}_k^*]_{N\text{-}K+1} & [\mathbf{u}_k^*]_{N\text{-}K+2} & \ldots & [\mathbf{u}_k^*]_N \\ [\mathbf{u}_k^*]_{N\text{-}K} & [\mathbf{u}_k^*]_{N\text{-}K+1} & \ldots & [\mathbf{u}_k^*]_{N\text{-}1} \\ \vdots & \vdots & \ddots & \vdots \\ [\mathbf{u}_k^*]_2 & [\mathbf{u}_k^*]_3 & \ldots & [\mathbf{u}_k^*]_{K+1} \end{bmatrix}_{(N\text{-}K,K)} \\ \mathbf{g}_{b_k} &= -\begin{bmatrix} [\mathbf{u}_k^*]_{N\text{-}K} & \cdots & [\mathbf{u}_k^*]_1 \end{bmatrix}^T_{((N\text{-}K),1)}\end{aligned} \tag{17}$$

So the following equations could be obtained from (17),

$$\begin{aligned}\mathbf{F}_B &= \begin{bmatrix} \mathbf{F}_{b_1}^T & \cdots & \mathbf{F}_{b_{N_r}}^T \end{bmatrix}^T_{(N_r(N\text{-}K),K)} \\ \mathbf{g}_B &= \begin{bmatrix} \mathbf{g}_{b_1}^T & \cdots & \mathbf{g}_{b_{N_r}}^T \end{bmatrix}^T_{(N_r(N\text{-}K),1)}\end{aligned} \tag{18}$$

So by FBLP,

$$\text{vec}\left(\mathbf{B}\begin{pmatrix}\mathbf{E}_s\\ \mathbf{J}\mathbf{E}_s^*\end{pmatrix}\right)=\mathbf{F}\mathbf{c}-\mathbf{g}=\mathbf{0}_{(2N_r(N\text{-}K),1)} \tag{19}$$

where

$$\begin{aligned}\mathbf{F}&=\begin{bmatrix}\mathbf{F}_F^T & \mathbf{F}_B^T\end{bmatrix}^T_{(2N_r(N\text{-}K),K)}\\ \mathbf{g}&=\begin{bmatrix}\mathbf{g}_F^T & \mathbf{g}_B^T\end{bmatrix}^T_{(2N_r(N\text{-}K),1)}\end{aligned} \tag{20}$$

with $\mathbf{J}\in\mathbb{C}^{N\times N}$ is the anti-identity matrix. The objective is to find vector $\mathbf{c}$

$$\mathbf{c}=\begin{bmatrix}c_1 & c_2 & \cdots & c_K\end{bmatrix}^T \tag{21}$$

which can be estimated by least squares (LS) solution,

$$\min_{\mathbf{c}}||\mathbf{F}\mathbf{c}-\mathbf{g}||_2=\min_{\mathbf{c}}||\hat{\mathbf{e}}_{fb}||_2 \tag{22}$$

Thus, the initial $\mathbf{c}$ by the LS solution is as follows,

$$\hat{\mathbf{c}}_{ls}=(\mathbf{F}^H\mathbf{F})^{-1}\mathbf{F}^H\mathbf{g} \tag{23}$$

Due to the noise, (19) is an approximation. The estimation $\mathbf{c}$ can be improved by the following weighted least squares (WLS) solution,

$$\hat{\mathbf{c}}_{wls}=(\mathbf{F}^H\mathbf{W}\mathbf{F})^{-1}\mathbf{F}^H\mathbf{W}\mathbf{g} \tag{24}$$

where

$$\mathbf{W}\cong\mathbf{T}_{FB}\otimes(\mathbf{B}\mathbf{B}^H)^{-1} \tag{25}$$

$$\mathrm{T}_{FB}=diag\left(\frac{\lambda_1^2}{\lambda_1+\hat{\sigma}^2},\ldots,\frac{\lambda_{N_r}^2}{\lambda_1+\hat{\sigma}^2},\frac{\lambda_1^2}{\lambda_1+\hat{\sigma}^2},\ldots,\frac{\lambda_{N_r}^2}{\lambda_{N_r}+\hat{\sigma}^2}\right) \tag{26}$$

where $\hat{\sigma}^2=\frac{tr(\hat{\mathbf{D}}_n)}{N-N_r}$, $\hat{\sigma}^2$ denotes the estimate of noise power. More details about the derivation of (25) and (26) are shown in the Appendix.

C. Resolvable Number of Coherent Sources Analysis

Due to the increasing dimension of $\mathbf{F}$, the resolvable number of coherent sources by FBLP-Mod-PUMA is bigger than that of Mod-PUMA. The proof is as follows. By (20), the dimension of $\mathbf{F}$ is $(2N_r(N\text{-}K),K)$, so $rank(\mathbf{F})=\min[2N_r(N\text{-}K),K]$. We have

$$K\le 2N_r(N-K) \tag{27}$$

$$K\le\frac{2N_r}{2N_r+1}N \tag{28}$$

While for Mod-PUMA, the dimension of $\mathbf{F}_F$ is $(N_r(N\text{-}K),K)$, so we obtain

$$K\le\frac{N_r}{N_r+1}N \tag{29}$$

Therefore whenever the sources are partially coherent or fully coherent, $N_r\ge 1$, FBLP-Mod-PUMA can solve more sources than Mod-PUMA.

D. Analysis of Computational Complexity

As indicated in (7), (24) and (25), the values of $\mathbf{c}$ and $\mathbf{W}$ are interdependent. Therefore, the FBLP-Mod-PUMA calculates $\mathbf{c}$ and $\mathbf{W}$ with the WLS solution.

Compared with the PUMA and Mod-PUMA, the dimensions of the matrices in FBLP-Mod-PUMA, i.e., $\mathbf{F}$, $\mathbf{g}$, $\mathbf{T}$ and $\mathbf{W}$ increase. Table I provides a comparison of the algorithm complexity of PUMA, Mod-PUMA and FBLP-Mod-PUMA. Consequently, the computational complexity for each iteration of the proposed method is higher due to the increased dimensions of the matrices.

TABLE I
COMPARISON OF COMPUTATIONAL COMPLEXITY BETWEEN THE CLASSICAL PUMA, THE MOD-PUMA, THE FBLP-MOD-PUMA

Equation	$\mathbf{W}$	$\mathbf{c}_{wls}$
PUMA	$\mathcal{O}\left(K(N\text{-}K)^3\right)$	$\mathcal{O}(2K^3(N\text{-}K)+2K^3(N\text{-}K)^2+K^3+K^2(N\text{-}K))$
Mod-PUMA	$\mathcal{O}\left(N_r(N\text{-}K)^3\right)$	$\mathcal{O}(2K^2N_r(N\text{-}K)+2KN_r^2(N\text{-}K)^2+K^3+KN_r(N\text{-}K))$
FBLP-Mod-PUMA	$\mathcal{O}\left(2N_r(N\text{-}K)^3\right)$	$\mathcal{O}(4K^2N_r(N\text{-}K)+8KN_r^2(N\text{-}K)^2+K^3+2KN_r(N\text{-}K))$

IV. SIMULATION RESULTS

The performance of DOA estimation of coherent sources with different algorithms is compared with simulated data. We consider a 10-half-wavelength spaced elements ULA receiving K coherent sources, where K is known. The number of snapshots is 50 and the number of Monte Carlo tests is 100. The iteration number of algorithms is 3. The remaining simulations use the same parameters unless otherwise specified. RMSE is used to assess the performance of the compared algorithms, which is defined as $RMSE=\left(\frac{1}{KI}\sum_{k=1}^{K}\sum_{i=1}^{I}\left(\hat{\theta}_{k,i}\text{-}\theta_k\right)^2\right)^{1/2}$, where $\hat{\theta}_{k,i}$ is the k^{th} estimated angle obtained from the i^{th} Monte Carlo test, θ_k is the k^{th} true angle.

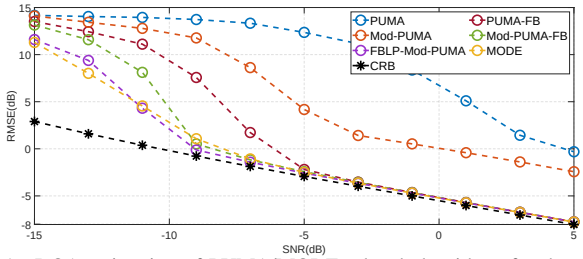

Fig. 1. DOA estimation of PUMA/MODE-related algorithms for three fully coherent sources from directions 1°, 8°, 35°

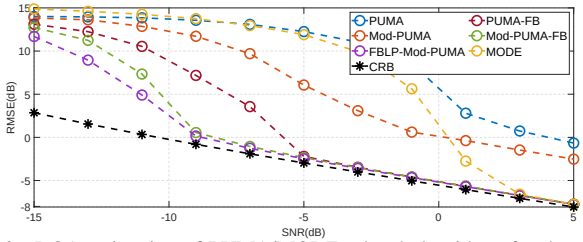

Fig. 2. DOA estimation of PUMA/MODE-related algorithms for three fully coherent sources from directions -25°, 2°, 9°

Fig. 1 and Fig. 2 show the RMSE performance comparison between PUMA, PUMA-FB, Mod-PUMA, Mod-PUMA-FB, FBLP-Mod-PUMA and MODE for 3 coherent sources from directions 1°, 8°, 35° and -25°, 2°, 9°, respectively. The performance of PUMA and Mod-PUMA are initially poor but improves significantly after applying the FBSS[1]. PUMA reconstructs the covariance matrix using $\mathbf{u}_1,\mathbf{u}_2,\ldots,\mathbf{u}_K$, while Mod-PUMA only uses $\mathbf{u}_1$, Mod-PUMA-FB utilizes $\mathbf{u}_1$ and

[1]FBSS is expressed by $\mathbf{\Gamma}_{fbss}=\frac{1}{2}(\mathbf{\Gamma}+\mathbf{J}\mathbf{\Gamma}^*\mathbf{J})$. FBSS can partially recover the rank of the covariance matrix in cases of $K\ge 3$ fully coherent sources.

$\mathbf{u}_2$. Compared to PUMA, Mod-PUMA shows a substantial improvement in low SNR regions. Notably, FBLP-Mod-PUMA, which does not employ FBSS and only uses $\mathbf{u}_1$ to reconstruct the signal subspace, shows a remarkable improvement of performance of low SNR regions, significantly outperforming PUMA and Mod-PUMA.

Furthermore, compared with Fig. 1 and Fig. 2, the performance of the MODE-related algorithms exhibits significant variation with different signal angles, whereas the performance of the PUMA-related algorithms remains relatively stable. This indicates that the PUMA-related algorithms, especially the FBLP-Mod-PUMA algorithm, demonstrate better robustness than the MODE-related algorithms, particularly in scenarios involving different signal angle configurations.

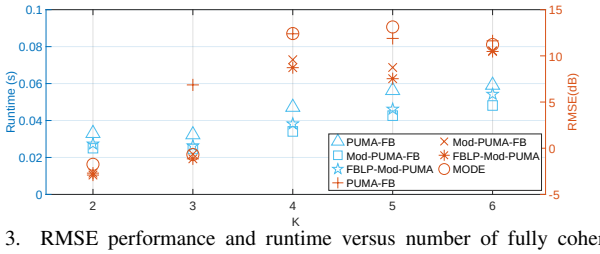

Fig. 3. RMSE performance and runtime versus number of fully coherent sources with SNR= -8dB

Fig. 3 shows the comparison of RMSE performance and runtime of different algorithms in terms of the number of coherent sources K with SNR = -8 dB. The simulation is realized on a system with Windows 11, i5-1340P, and Matlab R2023b. The y-axis on the right corresponds to the RMSE performance of various algorithms (markers in red), and the y-axis on the left corresponds to the runtime of various algorithms (markers in blue). For the comparison of RMSE performance, all the compared algorithms have similar performance for K=2, 3. However, as $K \geq 4$, the performance of MODE-related algorithms begins to deteriorate, while FBLP-Mod-PUMA maintains its robustness. This indicates that FBLP-Mod-PUMA exhibits superior robustness compared to MODE-related algorithms as the number of coherent sources increases. In particular, FBLP-Mod-PUMA consistently outperforms all other compared algorithms for all K values, demonstrating its effectiveness even in challenging low SNR cases. In terms of the algorithm's runtime, the histogram shows that PUMA has the longest runtime, followed by FBLP-Mod-PUMA, while Mod-PUMA has the shortest runtime. Moreover, the runtime of various algorithms increases as K increases, which is consistent with Table I.

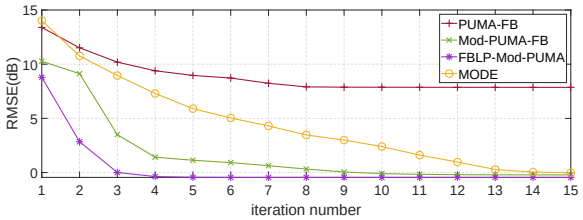

Fig. 4. RMSE performance versus iteration number, three fully coherent sources with 1°, 7°, 28°, SNR = -5dB

As shown in Fig. 4, the performance of all algorithms improves as the iteration number increases. When the iteration number exceeds 8, 10, 14, and 3 for PUMA-FB, Mod-PUMA-FB, MODE, and FBLP-Mod-PUMA, respectively, their RMSE performance is stable. Firstly, Mod-PUMA-FB only utilizes the eigenvectors associated with the N_r largest eigenvalues, $\mathbf{u}_1, \ldots, \mathbf{u}_{N_r}$ to reconstruct the signal subspace. As a result, compared to PUMA-FB, Mod-PUMA can achieve better performance with fewer iterations by avoiding the risk of mixing signal and noise eigenvectors [14]. Secondly, due to the extension by FBLP, the proposed FBLP-Mod-PUMA achieves better performance with fewer iteration numbers than Mod-PUMA-FB. In summary, compared with the other algorithms, the proposed FBLP-Mod-PUMA exhibits the fastest convergence speed and the best RMSE performance.

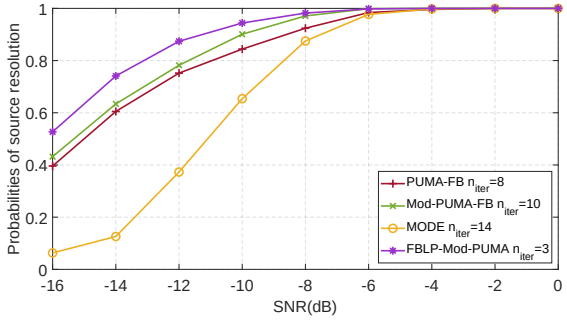

Fig. 5. Probabilities of source resolution with three fully coherent sources from directions 1°, 7°, 28°

The performance in terms of the probability of DOA resolution with three coherent sources from directions 1°, 7°, 28° is also evaluated. The DOAs are considered to be resolved if the following condition is satisfied $\left|\hat{\theta}_i - \theta_i\right| < \frac{\triangle\theta}{2}, i = 1, 2, 3$, where $\triangle\theta = min|\theta_m - \theta_n|, 1 \leq n < m \leq 3$. The number of iterations for PUMA-FB, Mod-PUMA-FB, MODE, and FBLP-Mod-PUMA, is 8, 10, 14, and 3, respectively. The number of Monte Carlo tests is 1000. As shown in Fig. 5, FBLP-Mod-PUMA consistently achieves the best performance in terms of the probability of DOA resolution compared to other PUMA-related and MODE-related algorithms.

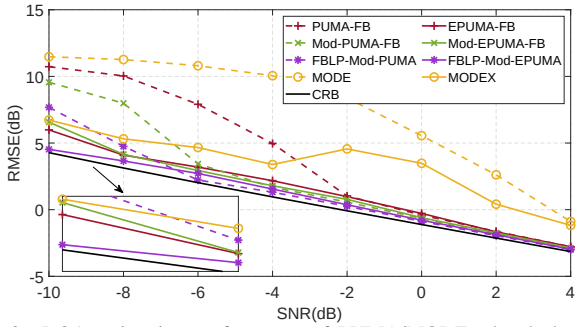

Fig. 6. DOA estimation performance of PUMA/MODE-related algorithms for six coherent sources from directions -35°, -7°, 1°, 8°, 35°, 50°

Fig. 6 shows the comparison of the DOA estimation performance of different algorithms in the case of six coherent sources from directions -35°, -7°, 1°, 8°, 35°, and 50°. These sources are divided into two incoherent groups, each containing three coherent signals. In this case, N_r=2, the RMSE performance of FBLP-Mod-PUMA shows a 3dB improvement over Mod-PUMA-FB, particularly in low SNR regions. FBLP-Mod-PUMA also exhibits superior performance in low SNR

regions, maintaining stability where other algorithms struggle, and performs slightly better than PUMA-FB and Mod-PUMA-FB in high SNR regions. Furthermore, the performance of EPUMA, Mod-EPUMA, FBLP-Mod-EPUMA, and MODEX improves significantly after applying a two-step selection strategy based on PUMA, Mod-PUMA, FBLP-Mod-PUMA, and MODE, respectively. For example, FBLP-Mod-EPUMA exhibits significant performance enhancements in low SNR regions.

V. Conclusion

This letter discusses the performance of PUMA-related and MODE-related algorithms in the presence of coherent signal sources. The proposed FBLP-Mod-PUMA/EPUMA is an extension of the Mod-PUMA/EPUMA algorithm based on FBLP. Notably, due to the integration of FBLP, the number of resolvable coherent sources of FBLP-Mod-PUMA is greater than the other PUMA-related algorithms. Simulation results show that the proposed FBLP-Mod-PUMA/EPUMA outperforms PUMA/EPUMA and Mod-PUMA/EPUMA, especially in low SNR regions, in terms of RMSE performance, convergence speed, and probability of source resolution.

Appendix

By the weighted least squares (WLS) solution [6],

$$\min_{\mathbf{c}} \hat{\mathbf{e}}_{fb}^{H}\mathbf{W}\hat{\mathbf{e}}_{fb} \tag{30}$$

$$\mathbf{W} = \left(E\left[\hat{\mathbf{e}}_{fb}\hat{\mathbf{e}}_{fb}^{H}\right]\right)^{-1} \tag{31}$$

$$\begin{aligned}\hat{\mathbf{e}}_{fb} &= \mathrm{vec}\left(\mathbf{B}\begin{pmatrix}\hat{\mathbf{E}}_s \\ \mathbf{J}\hat{\mathbf{E}}_s^*\end{pmatrix}\right) = \mathrm{vec}\left(\mathbf{B}\begin{pmatrix}\mathbf{E}_s+\triangle\mathbf{E}_s \\ \mathbf{J}(\mathbf{E}_s+\triangle\mathbf{E}_s)^*\end{pmatrix}\right)\\ &= \mathrm{vec}\left(\mathbf{B}\begin{pmatrix}\triangle\mathbf{E}_s \\ \mathbf{J}(\triangle\mathbf{E}_s^*)\end{pmatrix}\right) = (\mathbf{I}_K\otimes\mathbf{B})\begin{pmatrix}\triangle\mathbf{u}_s \\ \mathbf{J}_d(\triangle\mathbf{u}_s^*)\end{pmatrix}\end{aligned} \tag{32}$$

where $\hat{\mathbf{e}}_{fb} \in \mathbb{C}^{2N_r(N\text{-}K)\times 1}$, $\hat{\mathbf{E}}_s = \mathbf{E}_s + \triangle\mathbf{E}_s$, $\triangle\mathbf{u}_s = \mathrm{vec}(\triangle\mathbf{E}_s) = \left[\triangle\mathbf{u}_1{}^T, \ldots, \triangle\mathbf{u}_{N_r}{}^T\right]^T$, and $\mathbf{I}_K \in \mathbb{C}^{K\times K}$ is an identity matrix, $\mathbf{J}_d = diag\{\mathbf{J}, \ldots, \mathbf{J}\}$ is a diagonal matrix with N_r elements, each of them is $\mathbf{J}$, so

$$\mathbf{W} = \left[(\mathbf{I}_K\otimes\mathbf{B})E\left[\begin{pmatrix}\triangle\mathbf{u}_s \\ \mathbf{J}_d\triangle\mathbf{u}_s^*\end{pmatrix}\begin{pmatrix}\triangle\mathbf{u}_s \\ \mathbf{J}_d\triangle\mathbf{u}_s^*\end{pmatrix}^H\right](\mathbf{I}_K\otimes\mathbf{B})^H\right]^{-1} \tag{33}$$

Due to [15] $E\left[\triangle\mathbf{u}_i\triangle\mathbf{u}_j^H\right] \approx \frac{\eta_i}{M}\sum_{k=1,k\neq i}^{N}\frac{\eta_k}{(\eta_i-\eta_k)^2}\mathbf{u}_k\mathbf{u}_k^H\delta_{ij}$, where δ_{ij} is the delta function, η_i is the i^{th} largest eigenvalue of the covariance matrix $\mathbf{\Gamma}$ by (3), so

$$E\left[\begin{pmatrix}\triangle\mathbf{u}_s \\ \mathbf{J}_d\triangle\mathbf{u}_s^*\end{pmatrix}\begin{pmatrix}\triangle\mathbf{u}_s \\ \mathbf{J}_d\triangle\mathbf{u}_s^*\end{pmatrix}^H\right] = \begin{bmatrix}\mathbf{E}_1 & \mathbf{E}_2 \\ \mathbf{E}_3 & \mathbf{E}_4\end{bmatrix} \tag{34}$$

$$\begin{aligned}\mathbf{E}_1 &= diag\left(E[\triangle\mathbf{u}_1\triangle\mathbf{u}_1^H], \ldots, E[\triangle\mathbf{u}_{N_r}\triangle\mathbf{u}_{N_r}^H]\right)\\ \mathbf{E}_2 &= diag\left(E[\triangle\mathbf{u}_1\triangle\mathbf{u}_1^T\mathbf{J}], \ldots, E[\triangle\mathbf{u}_{N_r}\triangle\mathbf{u}_{N_r}^T\mathbf{J}]\right)\\ \mathbf{E}_3 &= diag\left(E[\mathbf{J}\triangle\mathbf{u}_1^*\triangle\mathbf{u}_1^H], \ldots, E[\mathbf{J}\triangle\mathbf{u}_{N_r}^*\triangle\mathbf{u}_{N_r}^H]\right)\\ \mathbf{E}_4 &= diag\left(E[\triangle\mathbf{u}_1^*(\triangle\mathbf{u}_1^*)^H], \ldots, E[\triangle\mathbf{u}_{N_r}^*(\triangle\mathbf{u}_{N_r}^*)^H]\right)\end{aligned} \tag{35}$$

According to [15], the sample eigenvectors are asymptotically complex normal, which indicated that $E[(\mathbf{u}_i+\triangle\mathbf{u}_i)(\mathbf{u}_i+\triangle\mathbf{u}_i)^T] - E[\mathbf{u}_i]E[\mathbf{u}_i]^T = 0$, and $E[\triangle\mathbf{u}_i\mathbf{u}_i^T] = E[\mathbf{u}_i\triangle\mathbf{u}_i^T] \approx 0$, so $E[\triangle\mathbf{u}_i\triangle\mathbf{u}_i^T] = -E[\triangle\mathbf{u}_i\mathbf{u}_i^T] - E[\mathbf{u}_i\triangle\mathbf{u}_i^T] \approx 0$, thus $\mathbf{E}_2 = \mathbf{E}_3 \approx \mathbf{0}$.

Therefore, (34) is a diagonal matrix written as $diag(\mathbf{E}_1, \mathbf{E}_4)$, which can be rewritten as (26) with $2N_r$ elements. Thus, (25) can be derived from (33) and (26).

Moreover, with the similar derivations as shown in Section IV "Perforamce analysis" of [8], the asymptotic variance of the FBLP-Mod-PUMA for DOA estimation is

$$E[(\triangle\theta_i)^2] \approx \frac{1}{2}\left(\frac{v}{2\pi d\cos\theta_i}\right)^2 E[|\triangle z_i|^2] \tag{36}$$

where $|\cdot|$ is the absolute value, $E[|\triangle z_i|^2] \approx \frac{\mathbf{z_i^T}(\mathbf{F^H W F})^{-1}\mathbf{z_i^*}}{|\alpha_i|^2}$, with $\mathbf{z}_i = [{z_i}^K \cdots 1]^T$, $\alpha_i = K{z_i}^{K-1} + (K-1)c_1{z_i}^{K-2} + \cdots + c_{K-1}$, v is the carrier wavelength, and $d = v/2$ is the inter-element spacing of the ULA.

References

[1] R. Schmidt, "Multiple emitter location and signal parameter estimation," in *IEEE Transactions on Antennas and Propagation*, vol. 34, no. 3, pp. 276-280, March 1986.

[2] R. Roy, A. Paulraj and T. Kailath, "ESPRIT-A subspace rotation approach to estimation of parameters of cisoids in noise," in *IEEE Transactions on Acoustics, Speech, and Signal Processing*, vol. 34, no. 5, pp. 1340-1342, October 1986.

[3] M. Sun, J. Pan, C. Le Bastard, Y. Wang and J. Li, "Advanced Signal Processing Methods for Ground-Penetrating Radar: Applications to Civil Engineering," in *IEEE Signal Processing Magazine*, vol. 36, no. 4, pp. 74-84, July 2019.

[4] P. Stoica and K. C. Sharman, "Maximum likelihood methods for direction-of-arrival estimation," in *IEEE Transactions on Acoustics, Speech, and Signal Processing*, vol. 38, no. 7, pp. 1132-1143, July 1990.

[5] A. B. Gershman and P. Stoica, "MODE with extra-roots (MODEX): a new DOA estimation algorithm with an improved threshold performance," *1999 IEEE International Conference on Acoustics, Speech, and Signal Processing. Proceedings. ICASSP99 (Cat. No.99CH36258)*, vol. 5, pp. 2833-2836, 1999.

[6] C. Qian, L. Huang, M. Cao, J. Xie and H. C. So, "PUMA: An Improved Realization of MODE for DOA Estimation," in *IEEE Transactions on Aerospace and Electronic Systems*, vol. 53, no. 5, pp. 2128-2139, Oct. 2017.

[7] H. C. So, F. K. W. Chan, W. H. Lau and C. -F. Chan, "An Efficient Approach for Two-Dimensional Parameter Estimation of a Single-Tone," in *IEEE Transactions on Signal Processing*, vol. 58, no. 4, pp. 1999-2009, April 2010.

[8] C. Qian, L. Huang, N. D. Sidiropoulos and H. C. So, "Enhanced PUMA for Direction-of-Arrival Estimation and Its Performance Analysis," in *IEEE Transactions on Signal Processing*, vol. 64, no. 16, pp. 4127-4137, Aug.15, 2016.

[9] D. Zachariah, P. Stoica and M. Jansson, "Comments on "Enhanced PUMA for Direction-of-Arrival Estimation and Its Performance Analysis"," in *IEEE Transactions on Signal Processing*, vol. 65, no. 22, pp. 6113-6114, Nov.15, 2017.

[10] T. Tang, C. Yang, T. Xie, Y. Liu, L. Xu and D. Chen, "FBC-SBL: Frequency Band Clustering Sparse Bayesian Learning for Off-Grid Wideband DOA Estimation With Different Frequency Bands," in *IEEE Geoscience and Remote Sensing Letters*, vol. 21, pp. 1-5, 2024.

[11] D. Xu, Y. Wang, J. Sarrazin, B. Ma and Q. Zhu, "DOA Estimation of Coherent Signals Based on EPUMA Method With Frequency Beam Scanning Leaky-Wave Antennas," in *IEEE Access*, vol. 11, pp. 88378-88387, 2023.

[12] D. Xu, Y. Wang, B. Ma, Q. Zhu and J. Sarrazin, "A Modified PUMA/EPUMA for Direction-of-Arrival Estimation of Coherent Sources," in *Digital Signal Processing*, vol. 158, https://doi.org/10.1016/j.dsp.2024.104967, 2025.

[13] P. Stoica and M. Jansson, "On forward–backward MODE for array signal processing," *Digital Signal Processing*, vol. 7, no.4, pp. 239-252, 1997.

[14] J. A. Cadzow, Y.S. Kim and D.C. Shiue, "General direction-of-arrival estimation: a signal subspace approach," in *IEEE Transactions on Aerospace and Electronic Systems*, vol. 25, no. 1, pp. 31-47, 1989.

[15] D. J. Jeffries, and D.R. Farrier, "Asymptotic results for eigenvector methods," in *IEE Proceedings F-Communications, Radar and Signal Processing*, vol. 7. no. 132, pp. 589-594, 1985.